Facile preparation of cellulose microfibers exfoliated graphite composite; A robust sensor for determination of dopamine in biological samples

Selvakumar Palanisamy[a, b], Pan Yi-Fan[a], Shen-Ming Chen[a]*, Vijayalakshmi Velusamy[b]**, James M. Hall[b]

[a]Electroanalysis and Bioelectrochemistry Lab, Department of Chemical Engineering and Biotechnology, National Taipei University of Technology, No. 1, Section 3, Chung-Hsiao East Road, Taipei 106, Taiwan.

[b]Division of Electrical and Electronic Engineering, School of Engineering, Manchester Metropolitan University, Manchester – M1 5GD, United Kingdom.

Corresponding authors

*S.M. Chen, E-mail: smchen78@ms15.hinet.net

**V. Velusamy, E-mail: V.Velusamy@mmu.ac.uk

Abstract

A simple and robust dopamine sensor was developed using cellulose microfibers (CMF) exfoliated graphite composite modified screen-printed carbon electrode (SPCE) for the first time. The graphite-CMF composite was prepared by sonication of pristine graphite in CMF solution and was characterized by high-resolution scanning electron microscopy, Fourier transform, infrared, and Raman spectroscopy. The cyclic voltammetry results reveal that graphite-CMF composite modified SPCE has superior electrocatalytic activity against oxidation of dopamine (DA) than SPCE modified with pristine graphite and CMF. The presence of large edge plane defects on exfoliated graphite and abundant oxygen functional groups of CMF enhance electrocatalytic activity and decrease potential towards the oxidation of DA. Differential pulse voltammetry was used to quantify the DA using graphite-CMF composite modified SPCE and demonstrates a linear response for DA detection in the range 0.06 to 134.5 µM. The sensor shows a detection limit as 10 nM with an appropriate sensitivity, and displays appropriate recovery of DA in human serum samples with good repeatability. Sensor selectivity is demonstrated in the presence of 50 fold concentrations of potentially active interfering compounds including ascorbic acid, uric acid, and dihydroxybenzene isomers.

Keywords: Exfoliated graphite; Cellulose microfibers; Functional composite; Dopamine; Electrochemical sensor

Introduction

Over the past two decades, the synthesis of novel composite materials has received substantial attention in electroanalytical chemistry and have shown great potential capacity and signal-enhancing characteristics in electroanalytical applications for sensing of small molecules (Shrivastava et al. 2016). Dopamine (DA) is an inhibitory neurotransmitter and plays an important role in human metabolism, and in the renal and central nervous systems (Pandikumar et al. 2014). Dysfunction of DA transmission in the substantia nigra of the central nervous system (CNS) are implicated in Parkinson's disease and schizophrenia (Mo and Ogorevc 2001; Galvan and Wichmann 2001). Accordingly, the real-time monitoring of DA concentrations in human tissue samples has received considerable interest. To date, a range of analytical methods has been employed for clinical DA determination (Palanisamy et al 2013). However, electrochemical techniques are ideally suited to the detection of DA due to their robustness with fast response, high sensitivity, stability and selectivity (Liu et al. 2008; Paleček 2002).

Composite modified electrodes have been widely used as transducers for detection of DA, and they demonstrate improved detection limit (LOD), sensitivity, and linear response over unmodified electrodes (Jackowska and Krysinski 2013). Although DA is a highly electroactive molecule, interactions with unmodified electrodes exhibit low sensitivity, poor selectivity, and surface fouling, effectively limiting their practical application in electrochemical sensing (Thirumalraj et al. 2016). Consequently, carbon nano/micro materials, metal nanoparticles, transition metal oxides, and conducting polymer-based composite modified electrodes (including carbon nanotubes, graphene and its derivatives) are widely applied for different potential applications including the determination of DA (Vellaichamy et al. 2017a; Vellaichamy and Prakash 2016; Vellaichamy et al. 2017b; Jacobs et al. 2010; Sajid et al. 2016; Yang et al. 2015).

Accordingly, the preparation of simple and robust composite materials for the detection of DA is of interest to the applied analytical chemists. As a low-cost carbon material, graphite has been widely used as a starting point for synthesis of graphene oxide and its derivatives (Özerol et al. 2015; Choi et al. 2010). However, the electrochemical application of pristine graphite is limited by its low surface area and strongly linked carbon atoms (Ku et al. 2013). Thus, a range of materials and preparative approaches have been developed enhance the synergistic properties of graphite. For instance, we have more recently demonstrated the preparation of carbohydrate polymers dispersed graphite as an alternative composite material to graphene based DA sensors (Ku et al. 2013; Palanisamy et al. 2016a; Palanisamy et al. 2016b; Gui et al. 2013; Ruiz-Palomero et al. 2017). On the other hand, cellulose based materials have emerged as a new biomaterial and exhibited extraordinary electronic and structural properties with low toxicity (Gui et al. 2013). Additionally, they have high surface area, high porosity, and tend to bond easily with the variety of conductive materials (Gui et al. 2013; Ruiz-Palomero et al. 2017). Recently published literatures indicate that nano and micro cellulosic materials act to exfoliate bulk graphite into layered graphite flakes, particularly multi-layer graphene (Carrasco et al. 2014; Malho et al. 2012). In addition, as a composite component, cellulose-exfoliated graphite confers significantly improved electronic properties over pristine graphite (Malho et al. 2012). In the present work, we demonstrate a simple preparation of cellulose microfibers exfoliated graphite (graphite-CMF) composite by sonication method.

Our literature survey indicates that cellulose exfoliated graphite composite has not been previously used in electrochemical sensor applications. Consequently, we have also utilized the special properties of graphite-CMF composite for electrochemical determination of DA for the first time. We have also discussed the relation of DA electro-oxidation by graphite-CMF

composite modified electrode with graphite and CMF modified electrodes. As a proof of concept, we have also utilized the fabricated sensor towards the determination of DA in human serum samples.

Experimental

Materials and methods

Raw graphite with an average diameter 10 µm was purchased from Sigma-Aldrich. Screen-printed carbon electrodes were purchased from Zensor R&D Co. Ltd, Taiwan. Cellulose medium fibers powder (10 microns) was obtained from Sigma and used as received. Dopamine hydrochloride and dopamine injections were received from Sigma-Aldrich. Human serum samples were obtained from Valley Biomedical, Taiwan product & services, and were approved by the ethics committee of Chang-Gung memorial hospital through the contract no.IRB101-5042A3. All the chemicals used in this work were of analytical grade and was purchased from Sigma-Aldrich. The supporting electrolyte was pH 7.0 phosphate buffer and was prepared using 0.05 M Na_2HPO_4 and NaH_2PO_4 in doubly distilled water. The stock solutions were prepared using the doubly distilled water.

The electrochemical studies such as cyclic voltammetry and differential pulse voltammetry (DPV) were performed using computerized CHI410A electrochemical workstation from CH instruments. High-resolution scanning microscopic images were obtained using Hitachi S-4300SE/N High Resolution Schottky Analytical VP scanning electron microscope (SEM). The elemental mapping of the materials was analyzed using Hitachi S-4300SE/N High Resolution Schottky Analytical VP SEM attached BRUKER AXS elemental analyzer. Raman spectrum of materials was acquired using Dong Woo 500i Raman spectrometer from Korea. Fourier transform infrared (FTIR) spectroscopy analysis was performed using JASCO FTIR-6600 spectrometer.

Electrochemical studies were accomplished using a typical three-electrode system consisting of a modified Screen-printed carbon electrode (SPCE) as the working electrode, and saturated Ag|AgCl and Pt wire as the reference and auxiliary electrodes, respectively. The geometric surface area of unmodified SPCE was 0.07 cm^2 and the electrochemically active surface area (ECAS) of the modified SPCE (graphite-CMF) was 0.106 cm^2.

Preparation of graphite-CMF *composite and electrode modifications*

The graphite-CMF composite was prepared by dispersing of 10 mg graphite into 2 mL CMF solution and ultrasonication for approximately 45 min. The CMF stock solution was prepared by sonication of 50 mg of CMF in 5 mL doubly distilled water for 45 min. The raw graphite dispersion was prepared by adding 5 mg of graphite to 1 mL of dimethylformamide and sonicated for 30 min. For electrode modifications, 9 µL (optimum, see **Fig. 4 inset**) of the as-prepared graphite-CMF composite dispersion was drop coated on unmodified SPCE. The resulting graphite-CMF composite modified SPCE was dried in air oven. The graphite and CMF modified SPCEs were prepared by drop coating of 5 µL of graphite and CMF on the unmodified SPCEs. The electrochemical measurements were performed in a room temperature under the oxygen-free atmosphere by purging pure N_2 in the electrolyte solution for 10 min. The modified SPCEs were stored at room temperature under dry conditions when not in use.

Results and discussion

Characterization of graphite-CMF composite

Fig. 1 displays the high-resolution SEM images of graphite (A) and graphite-CMF composite (B). The SEM image of graphite-CMF composite reveals that the surface of graphite layers is highly exfoliated and uniformly wrapped by CMF. Conversely, the SEM image of graphite shows its layered structure with highly ordered graphite microsheets. The high

magnification SEM image of graphite-CMF composite (**Fig. 1B inset**) also confirmed the exfoliation of graphite and presence of CMF on the surface of graphite; the strong non-covalent interaction between the graphitic carbons and the CMF resulting in exfoliation of graphite. In addition, the hydrophilicity nature of CMF allows the dispersion of graphite-CMF composite into the water (Carrasco et al. 2014; Malho et al. 2012). The elemental mapping of the SEM images of graphite and graphite-CMF composite is shown in **Fig. 1C** and **D**. The elemental mapping of graphite-CMF composite confirms the presence of carbon and oxygen due the presence of graphite and CMF. In contrast, oxygen is absent in the elemental mapping of pristine graphite, and confirms the pure carbon nature of pristine graphite. The above observations confirm formation of the graphite-CMF composite.

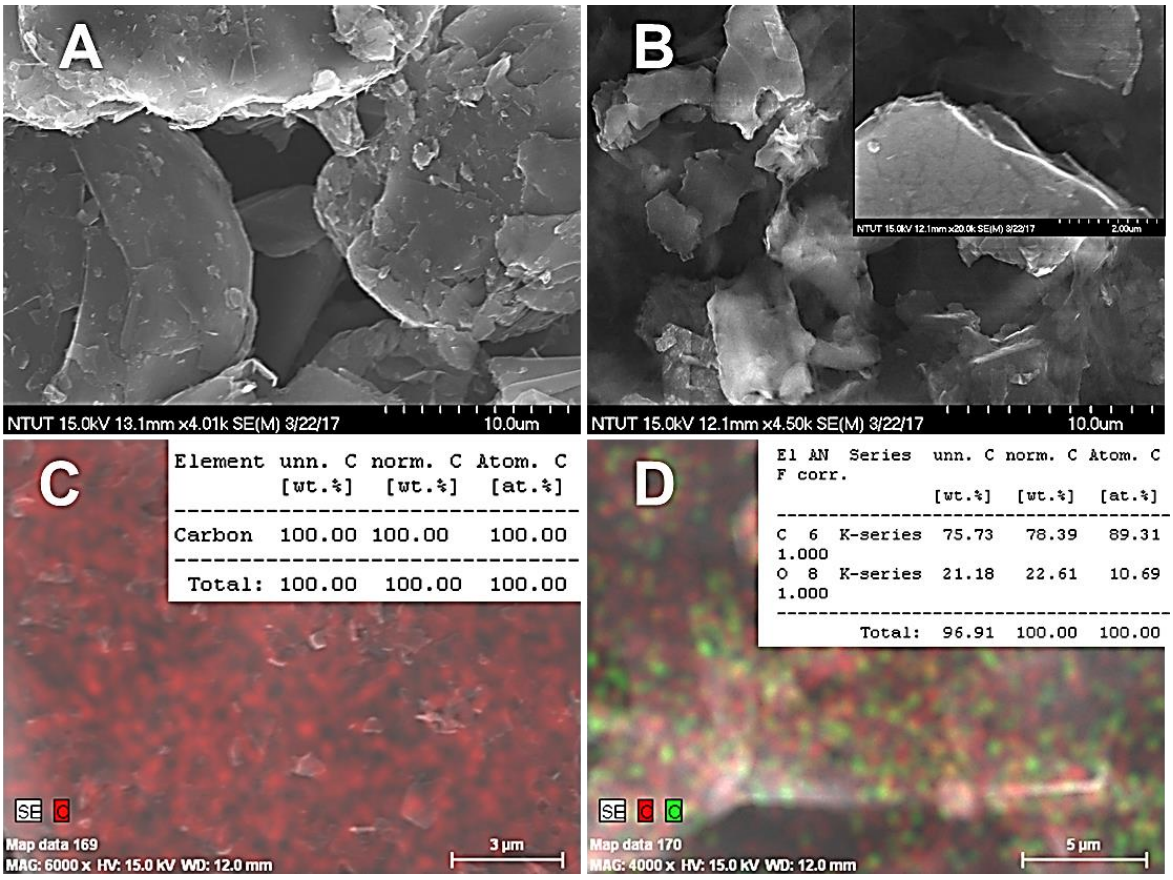

Raman spectroscopy is widely used as a standard tool to confirm the defects and disorders of carbon materials. **Fig. 2A** shows the Raman spectra of graphite (black color) and graphite-CMF composite (green color). The Raman spectrum of graphite shows a sharp G band at 1584 cm^{-1}, while D bands are absent in the Raman spectrum of graphite. This G band is associated with vibrations of the sp^2 domains of graphite (Thirumalraj et al. 2015). Alternatively, the Raman spectrum of graphite-CMF shows an intense D and G bands at 1336 and 1581 cm^{-1}. Typically, the appearance of D band vibrations is due to the presence of defects at the edges in pristine graphite and exfoliation bulk graphite into the multi-layered graphene (Malho et al. 2012). Accordingly, the result confirms that graphite-CMF composite has more edge detects than pristine graphite.

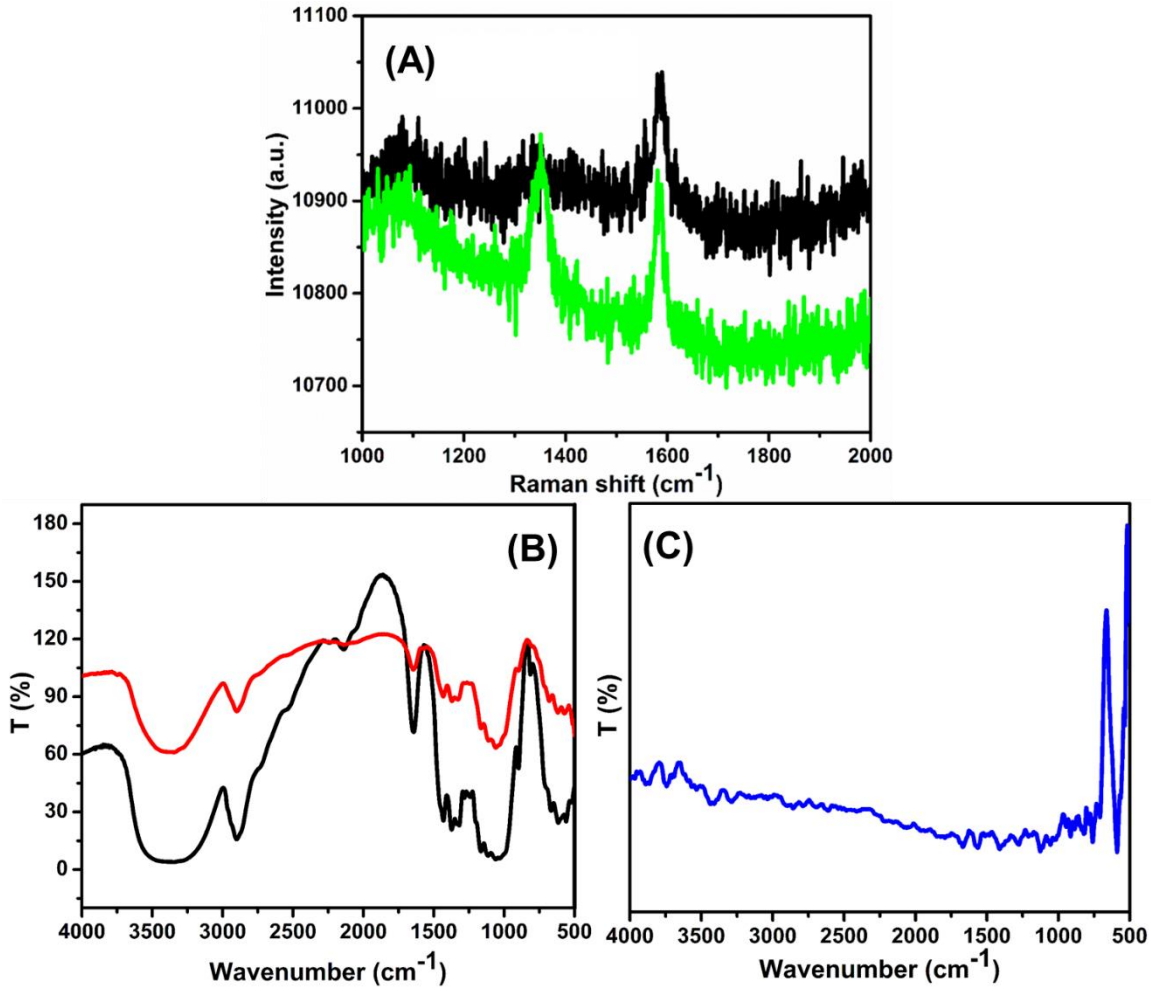

FTIR was used to characterize the presence of CMF and interactions between the CMF and graphite in the composite. **Fig. 2B** shows the FTIR spectra of CMF (red color) and graphite-CMF composite (black color,) and **Fig. 2C** shows the FTIR spectrum of graphite. A broad vibration band was detected at 3300–3500 cm^{-1} in graphite-CMF composite. This is due to the stretching vibrations of –OH group of CMF (Abdulkhani et al. 2013). The graphite-CMF composite also shows 2 additional bands at 2892 and 2220 cm^{-1}, which are associated with the stretching vibrations of –CH and $–CH_2$ from CMF (Abdulkhani et al. 2013). In addition, three characteristic bands were appeared at 1640, 1372 and 1058 cm^{-1}, are attributed to the vibrations of –OH, C=O and C–O from CMF (Abdulkhani et al. 2013). The similar characteristic stretching bands were observed for the FTIR spectrum of pure CMF. Conversely, the FTIR spectrum of graphite as shown in **Fig. 2C** do not show the obvious bands in the fingerprint region, and confirms the presence of pure carbon nature of graphite. The above results are more consistent with our previous reported literature for CMF and confirm the presence of CMF in graphene-CMF composite (Palanisamy et al. 2017).

Electrocatalytic ability of modified SPCEs towards DA

To investigate the electrocatalytic ability, the different modified SPCEs were tested by cyclic voltammetry (CV) in pH 7.0 containing 10 µM DA. **Fig. 3A** shows the CV response of bare (a), GR (b), CMF (c), CMF drop coated graphite (d) and graphite-CMF composite (e) modified SPCEs in 10 µM DA at pH 7.0 and at a scan rate of 50 mV/s. The unmodified SPCE did not show any obvious electrochemical response for the presence of DA, and reflects the poor electrocatalytic activity of unmodified SPCE towards DA. The graphite modified SPCE shows weak electrochemical redox behaviour towards DA and the oxidation peak of DA is appeared at 0.396 V and is due to the oxidation of DA to corresponding quinone. The oxidation mechanism of DA

168 at carbon modified electrodes is well studied and documented (Ku et al. 2013; Palanisamy et al.
169 2016a; Palanisamy et al. 2016b; Gui et al. 2013; Ruiz-Palomero et al. 2017). The electrochemical
170 redox behaviour of DA was enhanced upon the SPCE modified with CMF and the oxidation
171 potential of DA (0.286 V) was detected at a lower potential than with the graphite modified SPCE.
172 The results indicate that CMF has high catalytic activity and lower oxidation potential towards the
173 detection of DA than graphite modified electrode. The graphite-CMF composite SPCE shows 10
174 folds enhanced oxidation peak current to DA than CMF modified SPCE and the oxidation potential
175 of DA was 64 mV (0.224 V) lower than those observed at CMF modified SPCE. These results
176 demonstrate the higher DA electrocatalytic activity of graphite-CMF composite SPCE in
177 comparison to other modified SPCEs. The large defects at the edges of graphite and high
178 adsorption ability of CMF in the composite are the main reasons for enhanced sensitivity and low
179 oxidation potential towards the detection of DA than graphite and CMF modified electrodes. To
180 verify the enhanced catalytic activity of DA by edge plane effects of graphite in graphite-CMF
181 composite, the CMF was detected using pristine graphite modified SPCE and its response to DA
182 was analyzed. As can be seen from **Fig. 3A** curve d, the CMF coated pristine graphite modified
183 SPCE show 3.5 folds reduction in oxidation peak current response to DA than graphite-CMF
184 composite electrode. This result further indicates that the enhanced sensitivity of DA is due to the
185 presence of large edge plane effects of graphite in graphite-CMF composite and is in good
186 agreement with the Raman spectrum (**Fig. 2A** green profile).

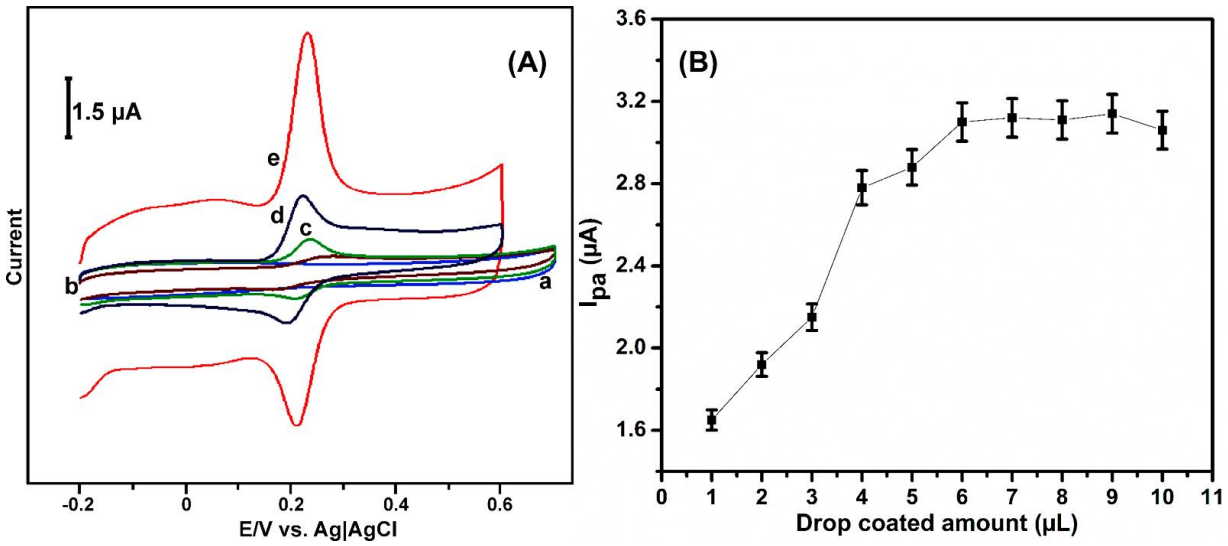

Optimization of the graphite-CMF composite towards the detection of DA is critical and has a direct influence on the sensitivity of the modified electrode. Accordingly, the effects on DA detection for differing volumes of graphite-CMF composite drop coated on modified SPCEs was studied by CV. The optimization results are shown in **Fig. 3B** and the experimental conditions are similar to **Fig. 3A**. The oxidation peak current response of DA can be clearly seen to increase alongside the volume of drop coated graphite-CMF composite on the SPCE surface. In addition, the response of DA was decreased above or below 9 µL drop coated graphite-CMF composite modified SPCE. Therefore, 9 µL drop coated graphite-CMF composite modified SPCE was used as an optimum of further electrochemical studies.

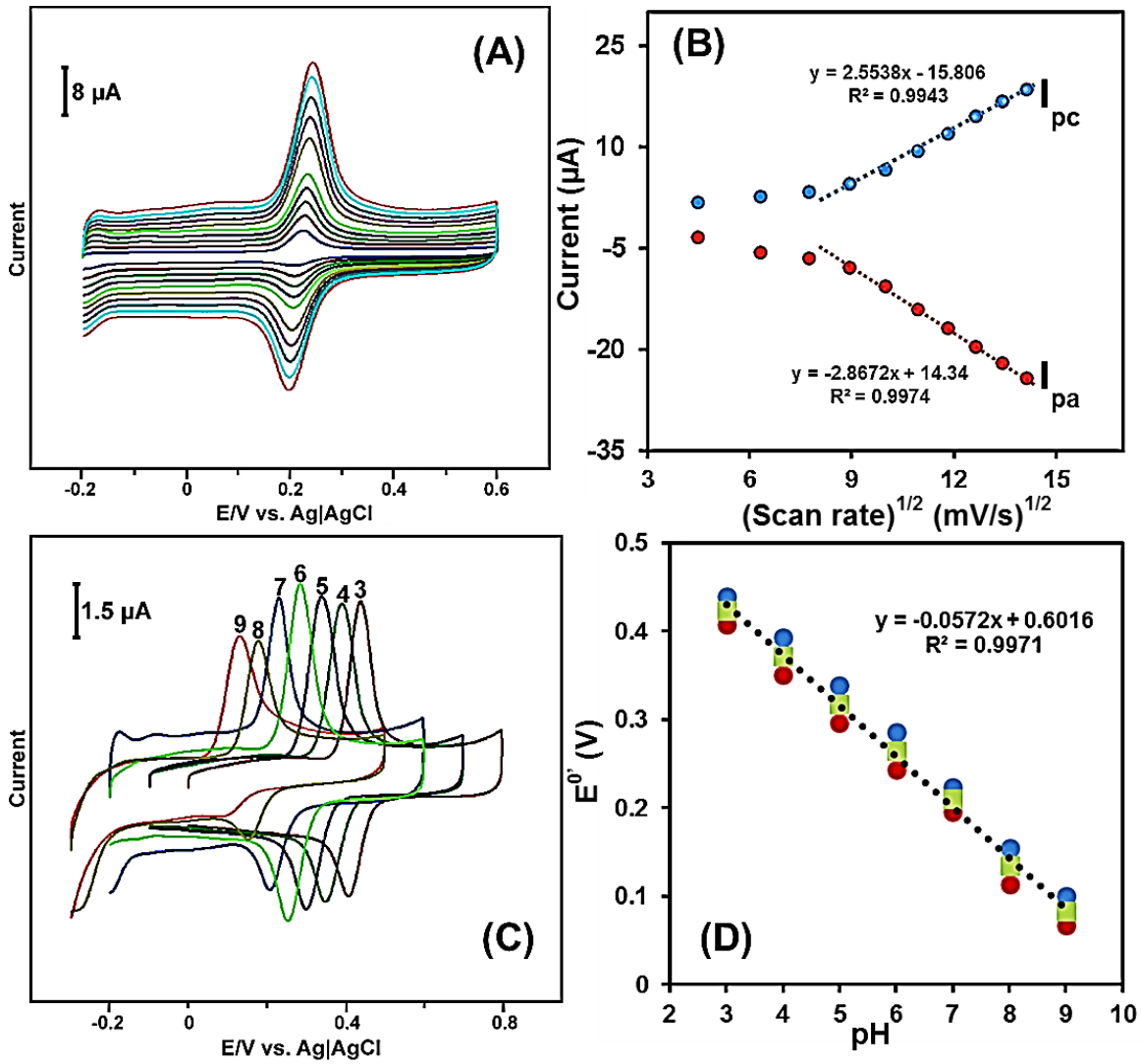

To verify the electrochemical behavior of DA, the effect of scan rate on the redox behavior of DA was studied. **Fig. 4A** shows the CVs of graphite-CMF composite modified SPCE in pH 7.0 containing 10 µM of DA at scan rates from 20 to 200 mVs^{-1}. The CV profile of graphite-CMF composite modified SPCE towards DA clearly demonstrate an increase in anodic and cathodic peak currents for DA with increasing scan rates. The corresponding anodic and cathodic peak currents vs. square root of scan rates were plotted and shown in **Fig. 4B**. The anodic and cathodic peak current of DA was linear over the scan rate from 90 to 200 mVs^{-1}, which suggests the electrochemical redox activity at the surface of graphite-CMF composite modified SPCE to be a

diffusion-controlled process at higher scan rates (Palanisamy et al. 2016a). However, as shown in **Fig. 4B**, the anodic and cathodic peak currents of DA exhibit a linear relationship to the scan rate and suggest the electrochemical redox behavior of DA at graphite-CMF composite modified SPCE to be an adsorption-controlled process at slow scan rates (Palanisamy et al. 2016a).

The influence of pH on the electrochemical redox behaviour of DA was investigated by CV. Over a pH range from pH 3 to PH 11, the electrochemistry of a graphite-CMF composite modified SPCE in 10 µM DA was investigated by CV at a scan rate of 50 mVs^{-1}. As shown in **Fig. 4C**, the graphite-CMF composite modified SPCE displays a well-defined redox couple for DA at each pH value, and the enhanced redox couple of DA were obtained at pH 3.0 to 7.0. In addition, the anodic (E_{pa}) and cathodic peak (E_{pc}) potential of DA shifted towards negative and positive direction upon increasing and decreasing the pH. The result indicates that protons are involved in the electrochemical redox reaction of DA at the graphite-CMF composite modified SPCE. As shown in **Fig. 4D**, the formal potential (defined as $(E_{pa} + E_{pc})/2$) of DA displays a linear relationship with pH over the range of pH 3 to pH 9, with a slope and correlation coefficient of 57.2 mV/pH and 0.9971, respectively. The slope value 57.2 mV/pH is very close to the theoretical slope value for an equal number of protons and electrons transferred electrochemical reaction (Palanisamy et al. 2016a). Hence, the electrochemical redox reaction of DA at graphite-CMF composite modified SPCE is involving of equal number of protons and electrons transferred electrochemical reaction. According to early reports, the electrochemical redox reaction of DA is involving the transfer of two protons and electrons, whereby DA is oxidised to quinone and subsequently reduced to DA (Palanisamy et al. 2016a; Palanisamy et al. 2016b).

Determination of DA

DPV was used for the determination of DA, due to its higher sensitivity and better resolution than other voltammetric methods (Palanisamy et al. 2016c). Under optimized experimental conditions, the DPV response of graphite-CMF composite modified SPCE for the absence and presence of different concertation of DA (0.06 to 144.5 μM) containing N_2 saturated pH 7.0 was examined and the obtained DPV results are shown in **Fig. 5A**. The graphite-CMF composite modified SPCEs do not show any obvious response in the absence of DA (bottom first DPV curve), while a clear oxidation peak response was observed at 0.186 V for the presence of 60 nM DA. The oxidation peak current response of DA increased with the addition of DA at pH 7.0. As shown in **Fig. 5A** inset, the oxidation peak current response of DA showed a linear relationship to [DA] 0.06 to 134.5 μM. The regression equation for current response vs. [DA] was i (μA) = 0.1317 + 0.1509 c (μM) with the correlation coefficient of 0.9947. The detection limit (LOD) for DA was calculated as 10 nM using the IUPAC recommendations. The sensitivity (defined as slope of calibration plot (0.1317)/ECAS (0.106 cm^2)) of the sensor was estimated to be 1.24 $\mu A \mu M^{-1}$ cm^{-2}. To explain the advantages and novelty of the sensor, the analytical parameters of the sensor was compared with existing DA sensors and comparative results are shown in Table 1. As can be seen that the fabricated DA sensor exhibited a lower LOD, higher sensitivity, and a wider linear range in the detection of DA than previously reported DA sensors using different composite modified electrodes (Palanisamy et al 2013; Palanisamy et al. 2016a; Palanisamy et al. 2016b; Shanbhag et al. 2017; Xu et al. 2017; Caetano et al. 2017; Rahman et al. 2017; Haldorai et al. 2017; Yang et al. 2017; Fang et al. 2017; Daemia et al. 2017; Wang et al. 2017; Zhang et al. 2017; Vellaichamy et al. 2017b). Accordingly, graphite-CMF composite modified SPCE represent an alternative sensitive catalyst for low-level detection of DA. Additionally, the developed DA sensor

can be prepared in short time, is less expensive and is highly stable when compared to previously reported DA sensors as shown in Table 1.

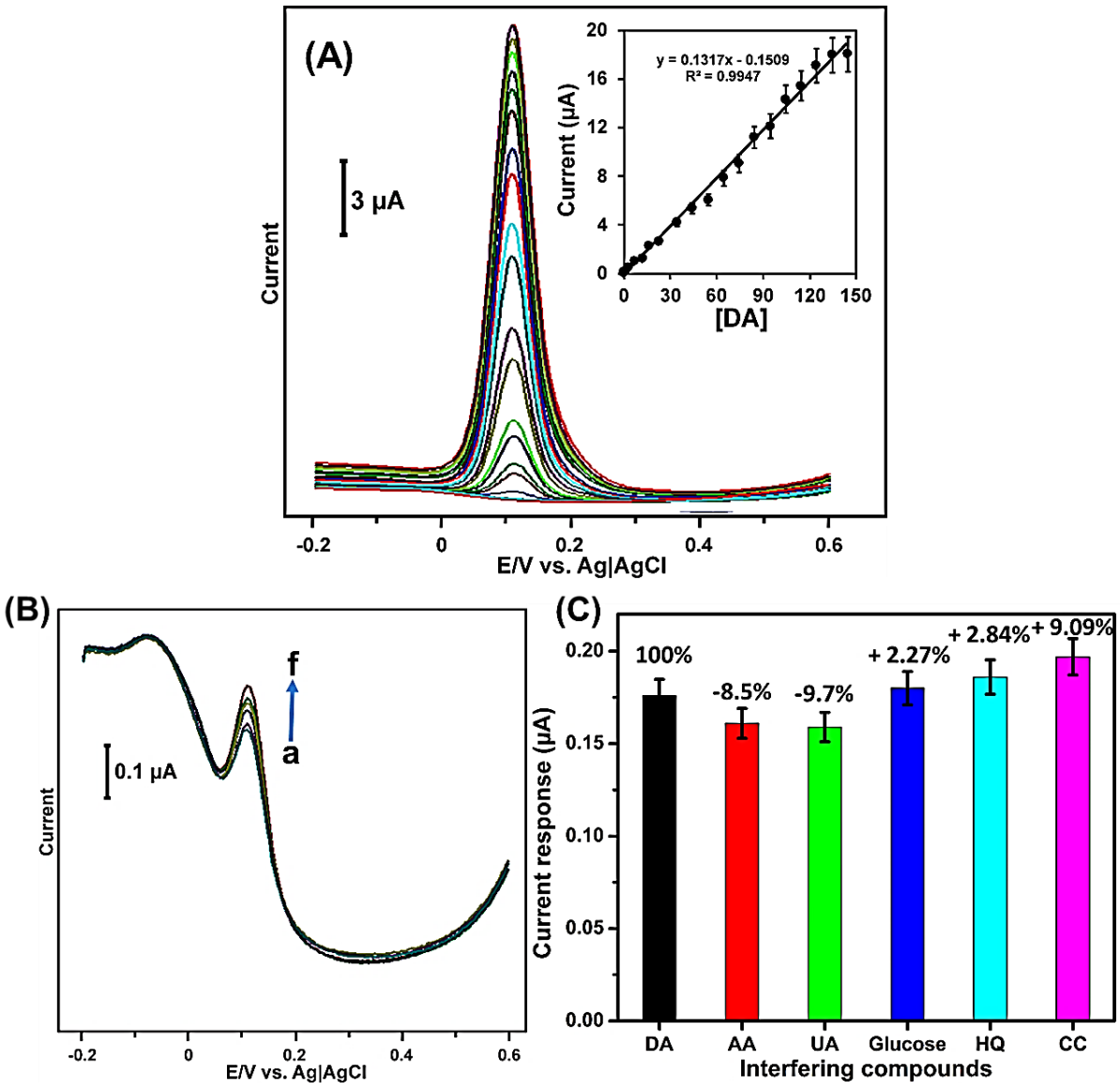

Selectivity of the sensor

To evaluate the selectivity of the sensor, the DA response of graphite-CMF composite modified SPCE was tested in the presence of potential interfering compounds. **Fig. 5B** shows the DPV response of graphite-CMF composite modified SPCE for the presence of 1 µM DA (c) and 50 µM additions of UA (a), AA (b), glucose (d), HQ (e) and CC (f) into PBS. The corresponding

current response change for DA for the presence of a 50 fold addition of interfering species are shown in **Fig. 5C**. It can be seen that the 50 fold addition of interfering species resulted in a limited effect (<10%) on the oxidation peak current response of DA at graphite-CMF composite modified SPCE due to the selective adsorption ability of DA by CMF. The developed sensor is therefore suited to the selective detection of DA in clinical samples.

D*etermination of DA in human serum samples*

To evaluate the practicality of the sensor, the graphite-CMF composite modified SPCE was used for the determination of DA in clinical human serum samples. The human samples were tested by the sensor and showed no detection of DA. The standard DA solution containing human serum samples was injected into the electrolyte solution and the recovery was calculated using standard addition method. The obtained recoveries of DA from human serum samples are shown in **Table 2**. In addition, the graphite-CMF composite modified SPCE shows an appropriate recovery (98.0 to 99.0%) with good repeatability (relative standard deviation = 3.4%) towards the determination of DA. The result indicates that graphite-CMF composite modified SPCE graphite-CMF composite modified SPCE can be used for the accurate detection of DA in biological samples.

Conclusions

In summary, we have demonstrated for the first time, a sensitive and robust DA electrochemical sensor based on graphite-CMF composite modified electrode. Physicochemical characterizations confirmed the exfoliation of bulk graphite into the multi-layered graphene and formation of graphite-CMF composite. Furthermore, the graphite-CMF composite modified electrode displayed higher electrocatalytic activity and lower oxidation potential towards the oxidation of DA than other modified electrodes. The fabricated sensor superior analytical features (high sensitivity, lower LOD and wide linear response range) towards the detection of DA than

previously reported DA sensors. The high selectivity and practicality of the sensor further authenticates its potential application in the determination of DA in clinical samples. Additionally, the sensor preparation is simple and less expensive when compared to currently available DA sensors.

Acknowledgments

This project was supported by the Ministry of Science and Technology, Taiwan (Republic of China). Authors are thankful to the department of Materials and Mineral Resources Engineering, National Taipei University of Technology for providing the high-resolution SEM and elemental mapping facility.

References

Abdulkhani A, Marvast EH, Ashori A et al (2013) Preparation of cellulose/polyvinyl alcohol biocomposite films using 1-n-butyl-3-methylimidazolium chloride. Int J Biol Macromol 62:379– 386.

Caetano FR, Felippe LB, Zarbin AJG et al (2017) Gold nanoparticles supported on multi-walled carbon nanotubes produced by biphasic modified method and dopamine sensing application. Sens Actuators B 243:43–50.

Carrasco PM, Montes S, Garcı´a I et al (2014) High-concentration aqueous dispersions of graphene produced by exfoliation of graphite using cellulose nanocrystals. Carbon 70:157–163.

Choi W, Lahiri I, Seelaboyin R et al (2010) Synthesis of graphene and its applications: A review. Crit Rev Solid State Mater Sci 35:52–71.

Daemia S, Ashkarrana AA, Baharia A et al (2017) Gold nanocages decorated biocompatible amine functionalized graphene as an efficient dopamine sensor platform. J Colloid Interface Sci 494:290–299.

Fang J, Xie Z, Wallace G et al (2017) Co-deposition of carbon dots and reduced graphene oxide nanosheets on carbon-fiber microelectrode surface for selective detection of dopamine. Appl Surf Sci 412:131–137.

Galvan A, Wichmann T (2008) Pathophysiology of parkinsonism. Clin Neurophysiol 119:1459–1474.

Gui Z, Zhu H, Gillette E et al (2013) Natural cellulose fiber as substrate for supercapacitor. ACS NANO 7:6037–6046.

Haldorai Y, Ezhil Vilian AT, Rethinasabapathy M et al (2017) Electrochemical determination of dopamine using a glassy carbon electrode modified with TiN-reduced graphene oxide nanocomposite. Sens Actuators B 247:61–69.

Jackowska K, Krysinski P (2013) New trends in the electrochemical sensing of dopamine. Anal Bioanal Chem 405:3753–3771.

Jacobs CB, Peairs MJ, Venton BJ (2010) Review: Carbon nanotube based electrochemical sensors for biomolecules. Anal Chim Acta 662:105–127.

Ku S, Palanisamy S, Chen S.M (2013) Highly selective dopamine electrochemical sensor based on electrochemically pretreated graphite and nafion composite modified screen printed carbon electrode. J Colloid Interface Sci 411:182-186.

Liu Y, Huang J, Hou H et al (2008) Simultaneous determination of dopamine, ascorbic acid and uric acid with electrospun carbon nanofibers modified electrode. Electrochem Commun 10:1431–1434.

Malho JM, Laaksonen P, Walther A et al (2012) Facile method for stiff, tough, and strong nanocomposites by direct exfoliation of multilayered graphene into native nanocellulose matrix. Biomacromolecules 13:1093−1099.

Mo JW, Ogorevc B (2001) Simultaneous measurement of dopamine and ascorbate at their physiological levels using voltammetric microprobe based on overoxidized poly(1,2-phenylenediamine)-coated carbon fiber. Anal Chem 73:1196–1202.

Özerol EA, Senkal BF, Okutan M (2015) Preparation and characterization of graphite composites of polyaniline. Microelectron Eng 146:76–80.

Palanisamy S, Ku S, Chen SM (2013) Dopamine sensor based on a glassy carbon electrode modified with a reduced graphene oxide and palladium nanoparticles composite. Microchim Acta 180:1037-1042.

Palanisamy S, Ramaraj SK, Chen SM et al (2017) A novel laccase biosensor based on laccase immobilized graphene-cellulose microfiber composite modified screen-printed carbon electrode for sensitive determination of catechol. Sci Rep 7:41214.

Palanisamy S, Sakthinathan S, Chen SM et al (2016a) Preparation of β-cyclodextrin entrapped graphite composite for sensitive detection of dopamine. Carbohydr Polym 135:267-273.

Palanisamy S, Thangavelu K, Chen SM et al (2016b) Preparation of chitosan grafted graphite composite for sensitive detection of dopamine in biological samples. Carbohydr Polym 151:401-407.

Palanisamy S, Thangavelu K, Chen SM et al (2016c) Preparation and characterization of gold nanoparticles decorated on graphene oxide@ polydopamine composite: application for sensitive and low potential detection of catechol. Sens Actuators B 233:298-306.

Paleček E (2002) Past, present and future of nucleic acids electrochemistry. Talanta 56:809–819.

Pandikumar A, How GTS, See TP et al (2014) Graphene and its nanocomposite material based electrochemical sensor platform for dopamine. RSC Adv 4:63296-63323.

Rahman MM, Lop NS, Ju MJ et al (2017) Highly sensitive and simultaneous detection of dopamine and uric acid at graphene nanoplatelet-modified fluorine-doped tin oxide electrode in the presence of ascorbic acid. J Electroanal Chem 792:54–60.

Ruiz-Palomero C, Soriano ML, Valcarcel M (2017) Nanocellulose as analyte and analytical tool: Opportunities and challenges. Trends Anal Chem 87:1–18.

Sajid M, Nazal MK, Mansha M et al (2016) Chemically modified electrodes for electrochemical detection of dopamine in the presence of uric acid and ascorbic acid: A review. Trends Anal Chem 76:15–29.

Shanbhag D, Bindu K, Aarathy AR et al (2017) Hydrothermally synthesized reduced graphene oxide and Sn doped manganese dioxide nanocomposites for supercapacitors and dopamine sensors. Mater Today Energy 4:66–74.

Shrivastava S, Jadon N, Jain R (2016) Next-generation polymer nanocomposite-based electrochemical sensors and biosensors: A review. Trends Anal Chem 82:55–67.

Thirumalraj B, Palanisamy S, Chen SM (2016) Alumina polished glassy carbon electrode as a simple electrode for lower potential electrochemical detection of dopamine in its sub-micromolar level. Electroanalysis 28:425–430.

Thirumalraj B, Palanisamy S, Chen SM et al (2015) Direct electrochemistry of glucose oxidase and sensing of glucose at a glassy carbon electrode modified with a reduced graphene oxide/fullerene-C60 composite. RSC Adv 5:77651-77657.

Vellaichamy B, Periakaruppan P, Ponnaiah SK (2017a) A new in-situ synthesized ternary CuNPs-PANI-GO nano composite for selective detection of carcinogenic hydrazine. Sens Actuators B 245:156-165.

Vellaichamy B, Periakaruppan P (2016) A facile in situ synthesis of highly active and reusable ternary Ag-PPy-GO nanocomposite for catalytic oxidation of hydroquinone in aqueous solution. J Catal 344:795-805.

Vellaichamy B, Periakaruppan P, Paulmony T (2017b) Evaluation of a New Biosensor Based on in Situ Synthesized PPy-Ag-PVP Nanohybrid for Selective Detection of Dopamine. J Phys Chem B 121:1118-1127.

Wang J, Yang B, Zhong J et al (2017) Dopamine and uric acid electrochemical sensor based on a glassy carbon electrode modified with cubic Pd and reduced graphene oxide nanocomposite. J Colloid Interface Sci 497:172–180.

Xu B, Su Y, Li L et al (2017) Thiol-functionalized single-layered MoS_2 nanosheet as a photoluminescence sensing platform via charge transfer for dopamine detection. Sens Actuators B 246:380–388.

Yang C, Denno ME, Pyakurel P et al (2015) Recent trends in carbon nanomaterial-based electrochemical sensors for biomolecules: A review. Anal Chim Acta 887:17–37.

Yang Z, Zheng X, Zheng J (2017) A facile one-step synthesis of Fe_2O_3/nitrogen-doped reduced graphene oxide nanocomposite for enhanced electrochemical determination of dopamine. J Alloys Compd 709:581–587.

Zhang YM, Xu PL, Zeng Q et al (2017) Magnetism-assisted modification of screen printed electrode with magnetic multi-walled carbon nanotubes for electrochemical determination of dopamine. Mate Sci Eng C 74:62–69.

393 **Table 1** Comparison of electroanalytical characteristics of graphite-CMF composite modified

394 SPCE with previously reported modified electrodes for determination of DA.

Modified electrode	LOD (μM)	Linear range (μM)	Sensitivity ($\mu A \mu M^{-1} cm^{-2}$)	Reference
[1]RGO-PdNPs/GCE	0.233	1–150.0	2.62	Palanisamy et al. 2013
[2]GR-CD/SPCE	0.011	0.1-58.5	1.27	Palanisamy et al. 2016a
[3]GR-CS/SPCE	0.0045	0.03-20.06	6.60	Palanisamy et al. 2016b
[4]Sn@rGO-MnO_2 NWs/GCE	0.13	0.1-350.0	4.334	Shanbhag et al. 2017
[5]TGA-MoS_2/GCE	0.027	0.05-20.0	Not reported	Xu et al. 2017
[6]MWCNT/GNPs/GCE	0.071	0.48-5.7	2.06	Caetano et al. 2017
[7]GNP/FTO	0.22	30.0-100.0	0.15	Rahman et al. 2017
[8]RGO-TiN/GCE	0.012	0.1-80.0	35.8	Haldorai et al. 2017
[9]Fe_2O_3/N-rGO/GCE	0.49	0.5-340.0	0.42	Yang et al. 2017
[10]CD/GO/CF	0.02	0.1-100.0	0.0065	Fang et al. 2017
[11]GNCs/CMG/GCE	0.028	0.1-80.0	Not reported	Daemia et al. 2017
[12]Pd/RGO/GCE	0.18	0.45-421.0	Not reported	Wang et al. 2017
[13]mMWCNTs/SPCE	0.43	5.0-180.0	Not reported	Zhang et al. 2017
[14]PPy-Ag-PVP/GCE	0.0126	0.01-0.09	0.0726	Vellaichamy et al. 2017b
Graphite-CMF/SPCE	0.01	0.06-134.5	1.24	This work

395

396 [1]RGO-PdNPs/GCE – Reduced graphene oxide-palladium nanoparticles composite modified

397 glassy carbon electrode

398 [2]GR-CD/SPCE – Graphite-cyclodextrin composite modified screen-printed carbon electrode

399 [3]GR-CS/SPCE – Graphite-chitosan composite modified screen-printed carbon electrode

400 [4]Sn@rGO-MnO_2 NWs/GCE – Hydrothermally synthesized reduced graphene oxide and Sn doped
401 manganese dioxide nanowires modified glassy carbon electrode
402 [5]TGA-MoS_2/GCE – Thiol-functionalized single-layered MoS_2 nanosheet modified glassy carbon
403 electrode
404 [6]MWCNTs/GNPs/GCE – Multiwalled carbon nanotubes and gold nanoparticles modified glassy
405 carbon electrode
406 [7]GNP/FTO – Gold nanoparticles modified fluorine doped oxide electrode
407 [8]RGO-TiN/GCE – Reduced graphene oxide and titanium nitride modified glassy carbon electrode
408 [9]Fe_2O_3/N-rGO/GCE – Iron oxide and nitrogen doped reduced graphene oxide modified glassy
409 carbon electrode
410 [10]CD/GO/CF – Carbon dots and graphene oxide modified carbon fiber
411 [11]GNCs/CMG/GCE – Gold nanocages decorated chemically modified graphene oxide modified
412 glassy carbon electrode
413 [12]Pd/RGO/GCE – Palladium nanoparticles and reduced graphene oxide modified glassy carbon
414 electrode
415 [13]mMWCNTs/SPCE – Magnetic multiwalled carbon nanotubes modified glassy carbon electrode
416 [14]PPy-Ag-PVP/GCE – Polypyrrole-silver-polyvinylpyrrolidone modified glassy carbon electrode
417
418

Table 2 Determination of DA in human serum samples using graphite-CMF composite (n = 3).

Sample	Detected (μM)	Added (μM)	Found (μM)	Recovery (%)	RSD* (%)
Human serum	0.0	2.0	1.98	99.0	**3.1**
		2.0	1.96	98.0	**3.7**

*Relative standard deviation for three measurements

Figure captions

Fig. 1 High-resolution SEM images of graphite (A) and graphite-CMF composite (B). Inset of B is the magnified SEM image of graphite -CMF composite. The elemental mapping of graphite (C) and graphite-CMF composite (D).

Fig. 2 A) Raman spectra of graphite (black color) and graphite-CMF composite (green color). B) FTIR spectra of CMF (red color) and graphite-CMF composite (black color). C) FTIR spectrum of graphite.

Fig. 3 A) Cyclic voltammetry response of bare (a), GR (b), CMF (c), CMF drop coated graphite (d) and graphite-CMF composite (e) modified SPCEs in 10 µM DA containing pH 7.0 at a scan rate of 50 mV/s. B) Effect of drop coating amount of graphite-CMF composite on SPCE vs. DA oxidation current response. The experimental conditions are similar to Fig. 3A.

Fig. 4 A) Cyclic voltammograms obtained for graphite-CMF composite modified SPCE in pH 7.0 containing 10 µM of DA at different scan rates. Inner to outer shows the scan rates from 20 to 200 mVs^{-1}). B) Calibration plot of square root of scan rate vs. I_{pa} and I_{pc} of DA. C) Cyclic voltammograms obtained for graphite-CMF composite coated SPCE for 10 µM of DA containing different pH, pHs were tested in the ranging from 3 to 9 at a scan rate of 50 mVs^{-1}. D) Calibration plot for pH vs. E^0.

Fig. 5 A) DPV response of graphite-CMF composite modified SPCE in the absence and presence of different concentration additions of DA (0.06 to 144.5 µM) into the N_2 saturated pH 7.0 Inset shows the linear calibration plot for DPV current response vs. [DA]. B) C) DPV response of graphite-CMF composite modified SPCE for the presence of 1 µM DA (c) and 50 µM additions of UA (a), AA (b), glucose (d), HQ (e) and CC (f) into PBS. C) The corresponding results for the effect of 50 folds addition of interfering species vs. DA current response change.